Supporting Information For:

Electrochemical Surface Interrogation of MoS_2 Hydrogen Evolving Catalyst: *In-situ* Determination of the Surface Hydride Coverage and the Hydrogen Evolution Kinetics

Hyun S. Ahn and Allen J. Bard*

Contribution from the Center for Electrochemistry, Department of Chemistry, The University of Texas at Austin, Austin, Texas 78712, United States

Email: ajbard@mail.utexas.edu

Experimental

General. All solutions were prepared using a Milli-Q deionized water (18.2 MΩ·cm, 4 ppb total oxidizable carbon). Sodium perchlorate (> 98%, Aldrich), anhydrous potassium phosphate monobasic (99% Fisher), anhydrous potassium phosphate dibasic (99% Fisher), 1,1'-ferrocenedimethanol (FcDM, 98%, Acros), and ammonium tetrathiomolybdate (99.97%, Aldrich) were used as received. Gold wire (99.99+%) of 25 µm diameter was purchased from Goodfellow (Devon, PA). The gold wire was used to fabricate the SECM tips as described elsewhere.[1] Unless otherwise specified, all electrodes used exhibited an RG (RG = [radius of the electrode plus the glass sheath] / [radius of the electrode]) of *ca.* 1.3 and were polished with alumina paste on microcloth pads prior to use. The surface of the electrodes were cleaned with an acidic piranha solution (1:1 v/v 40% H_2O_2 and concentrated H_2SO_4) before the experiments. The amorphous MoS_2 hydrogen evolving catalyst films were electrochemically deposited onto a gold SECM tip (substrate electrode) by a method described in the literature (also see page S2 below).[2] For all electrochemical measurements a Ag/AgCl reference electrode and a platinum wire counter electrode were used. The redox mediator solution was prepared freshly before each titration experiment and used for no more than 48 h.

Instrumentation. SECM experiments were conducted utilizing a CHI920D SECM station bipotentiostat and its built-in software (CH Instruments; Austin, TX). A rapid switching device for the fast SI-SECM titration experiments that was introduced recently[3] was employed in this work. Chronoamperometry (CA) was chosen as a detection technique in the SI-SECM experiments. The tip and the substrate electrodes (both 25 µm Au UME) were positioned at *ca.* 2.4 µm from one another, a distance at which generation-collection efficiency was unity (see below). For each data point collected, the substrate was stepped to E_{Subs} for a time t_{step} = 5 s followed by a potential step back to open circuit. A respective detection by stepping the potential of the tip was performed after a delay time t_{delay}. A total collection time of 15 s was selected for CA experiments. The redox mediator solutions employed in this work consisted of 1.6 mM 1,1'-ferrocenedimethanol in a pH 4.6 ± 0.3 potassium phosphate buffered water (0.1 M buffer strength).

SI-SECM tip-substrate alignment and approach

The tip-substrate alignment for the SI-SECM experiments was performed as described in literature precedents.[3-6] As in the previous cases, the substrate electrode remained stationary for the entire duration of the experiments and the tip electrode was positioned using a set of inchworm stepper motors and piezo controllers in the CHI920D SECM. As shown in Figure S1C, the tip-substrate alignments in the X and Y dimensions were achieved by current feedback response arising from the substrate reduction of the tip-oxidized $FcDM^+$. Because the substrate MoS_2 was poised to potentials negative enough for HER to occur, occasional bubble formation and loss of feedback occurred (Figure S1D). Tip-substrate approach was performed in the negative feedback mode (Figure S1A), unlike in the previous SI-SECM cases,[3-6] because of the H_2 bubble formation and loss of contact in positive feedback mode. By the negative feedback approach in the Z direction, the tip was placed at a distance of *ca.* 2.4 µm from the substrate, where quantitative generation-collection occurred (Figure S1B).

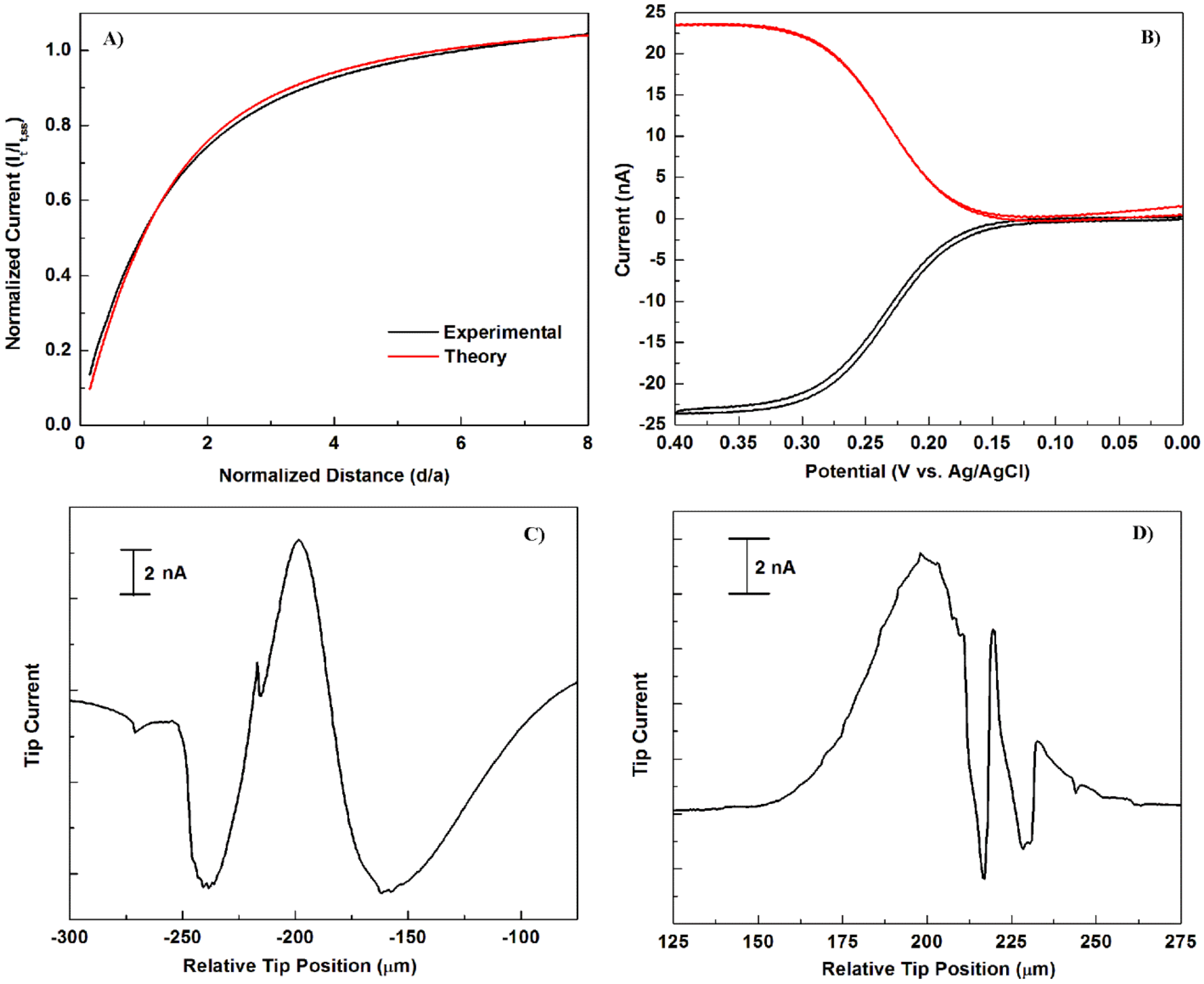

Figure S1. A) A negative feedback approach curve showing the tip current as a function of tip-substrate distance in the Z-direction – a tip-substrate gap of *ca.* 2.4 µm was confirmed by this method. **B)** A generation-collection CV at the 2.4 µm tip-substrate gap. Shown in red is the CV of tip oxidation of FcDM to $FcDM^+$. Black trace displays the reduction of tip-generated $FcDM^+$ back to FcDM at the substrate electrode. The currents in the two CVs are equal in magnitude and opposite in sign, confirming the quantitative substrate collection of the tip generated redox molecules. Solution contained 1.6 mM FcDM in a 0.1 M potassium phosphate buffered water at pH 4.6. **C)** A typical tip scan in the X-direction. A current drop due to the negative feedback coming from the glass sheath of the electrode, followed by the positive feedback from the substrate electrode reaction are displayed. This method was used to locate the substrate electrode and align the tip-substrate in the X and the Y directions. **D)** A tip scan in the Y-direction, similar to that shown in Figure S1C. Intermittent current losses due to H_2 bubble formation were observed.

Amorphous MoS_2 catalyst film deposition on a substrate UME

An amorphous film of MoS_2 was deposited on a 25 µm Au UME by a previous published method.[2] As seen in Figure S2, cyclic voltammetry was used as a deposition technique in a electrolyte bath containing 2 mM $(NH_4)_2MoS_4$ and 0.1 M $NaClO_4$. A 25 cycle deposition was performed, yielding a film of *ca.* 100 nm thickness.[2] The MoS_2 deposited Au UME was evaluated electrochemically for the surface coverage. Figure S3 exhibited that the MoS_2 deposited UME had little exposed area of the underlying Au electrode, evidenced by a negligible level of Faradaic current for FcDM oxidation in water. The MoS_2 deposited UME showed good HER catalysis, far superior to that of a gold UME (Figure S4).

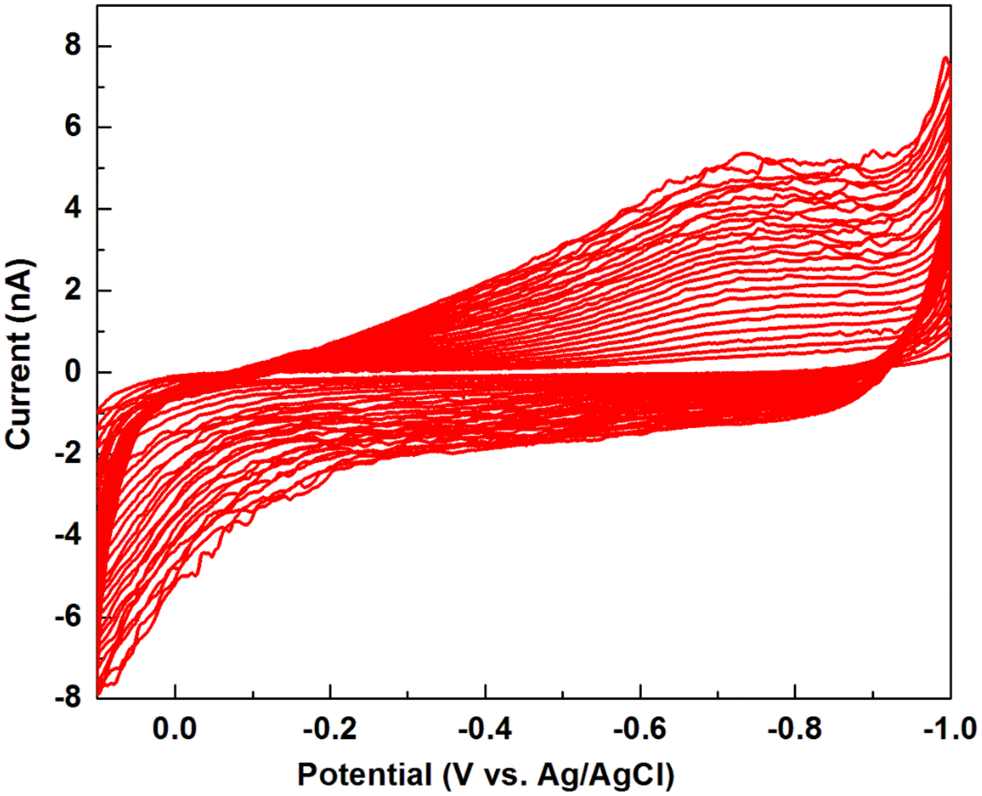

Figure S2. A cyclic voltammogram of the deposition process of MoS_2 on a 25 µm Au UME. The electrolyzing bath contained 2 mM $(NH_4)_2MoS_4$ and 0.1 M $NaClO_4$ in deionized water. Reduction of the Mo^{VI} in the bath to Mo^{IV}, followed by partial oxidation of the deposited film was cycled 25 times. Sequential growth of the film was evidenced in the increased current in the voltammogram. The cycling of potential ended at the reducing extreme of the potential range, at -1.0 V. Wave-like noise in the voltammogram is due to the slight disturbance in the solution arising from deaeration. The solution was constantly deaerated by bubbling Ar gas through in order to prevent oxidation of the MoS_2 film.

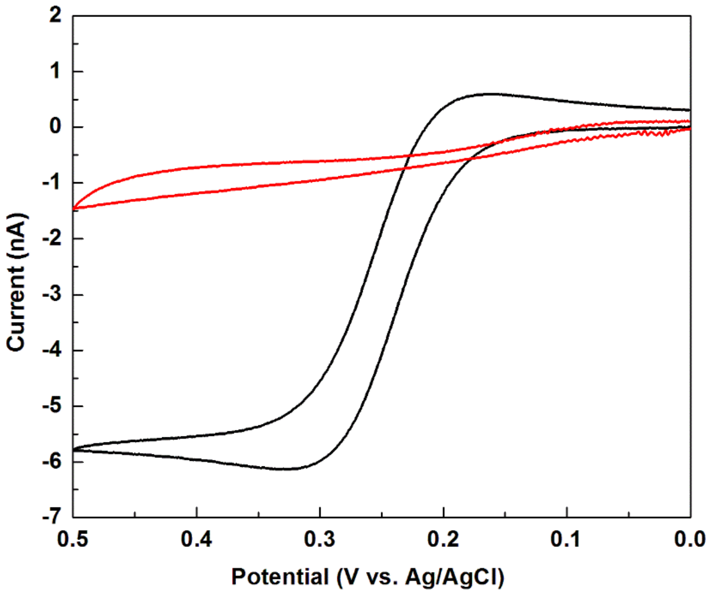

Figure S3. Cyclic voltammograms arising from the oxidation of 1.8 mM FcDM to $FcDM^+$ in pH 7 phosphate buffered water (Scan rate 50 mV/s). Black trace is that of a clean 25 µm Au UME, and red trace is that of a MoS_2 deposited 25 µm Au UME. MoS_2 deposition covered the underlying Au UME completely, evidenced by the negligible Faradaic current in the deposited electrode.

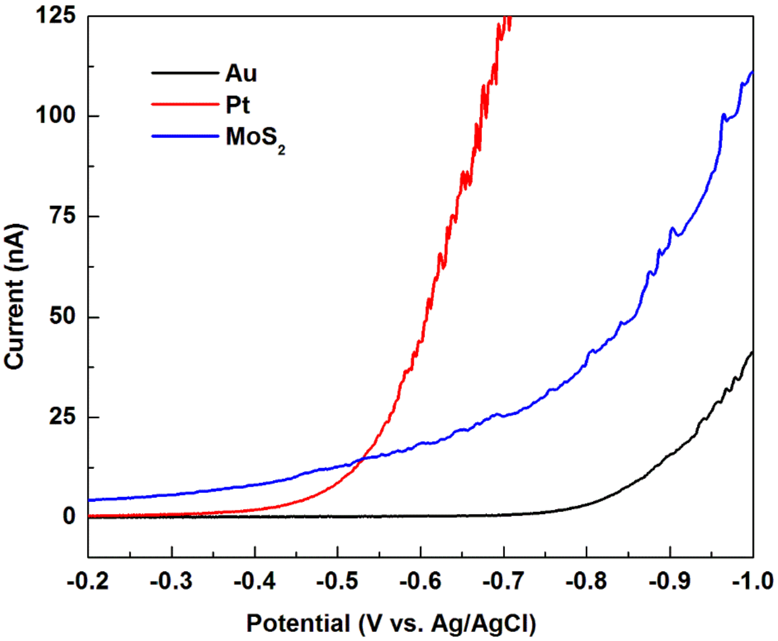

Figure S4. Linear sweep voltammograms of HER (0.1 M potassium phosphate, pH 5.3, scan rate 10 mV/s) on three 25 µm UME surfaces: Au (black), Pt (red), and MoS_2 (blue). The MoS_2 electrode exhibited good HER catalysis compared to that of the Au electrode. The MoS_2 HER overpotential over that of Pt was similar to that reported in the literature.[2] The reduction current in the MoS_2 voltammogram in the pre-HER potential range (-0.2 V to - 0.6 V) is attributed to the residual MoS_3 reduction.[2]

Capacitance measurement of the MoS_2 electrode

Electrochemical double layer capacitance measurement was performed on the MoS_2 electrode in order to gauge the roughness and porosity of the amorphous MoS_2 surface compared to other amorphous catalyst materials of known surface roughness such as the CoP_i oxygen evolving catalyst.[5,7] As shown in Figure S5, a set of capacitive charging experiments was performed at a non-Faradaic potential range at varying scan rates. The obtained currents were plotted as a function of scan rates in order to obtain the capacitive double layer charge according to the following equation:

$$C_{dl} = \frac{d_i}{d(\frac{\partial E}{\partial t})}$$

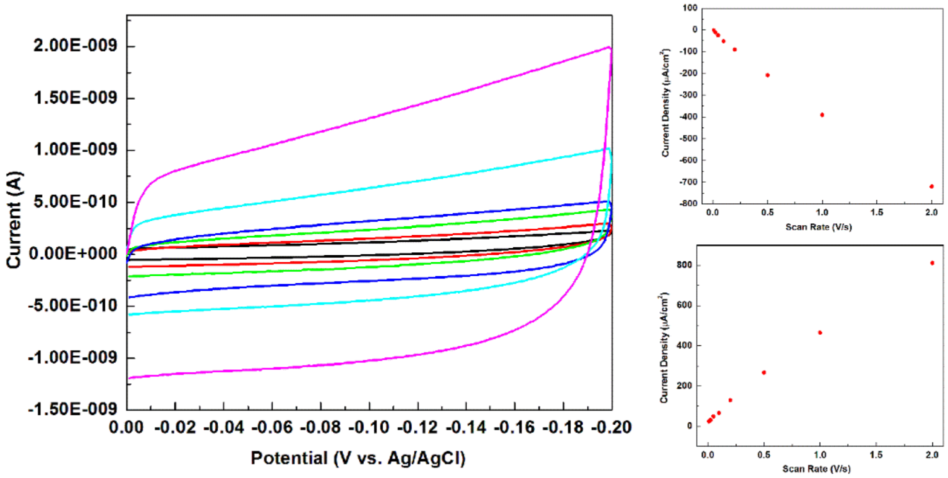

Figure S5. Cyclic voltammograms of non-Faradaic charging of the MoS_2 electrodes at varying scan rates from 10 mV/s to 2 V/s. Charging currents (two figures on the right) were plotted as a function of scan rate (for both forward and backward scans) to yield the double layer capacitance as the slope.

From the data, double layer capacitance of the MoS_2 electrode was calculated to be 360 ± 48 $\mu F/cm^2$. A typical capacitance for a smooth oxide/chalcogenide surface is *ca.* 60 $\mu F/cm^2$,[8] therefore the roughness factor of the MoS_2 electrode is 6. This roughness factor is much higher than that observed for another type of amorphous catalyst surface, CoP_i, which was measured at 2.3.[5,7]

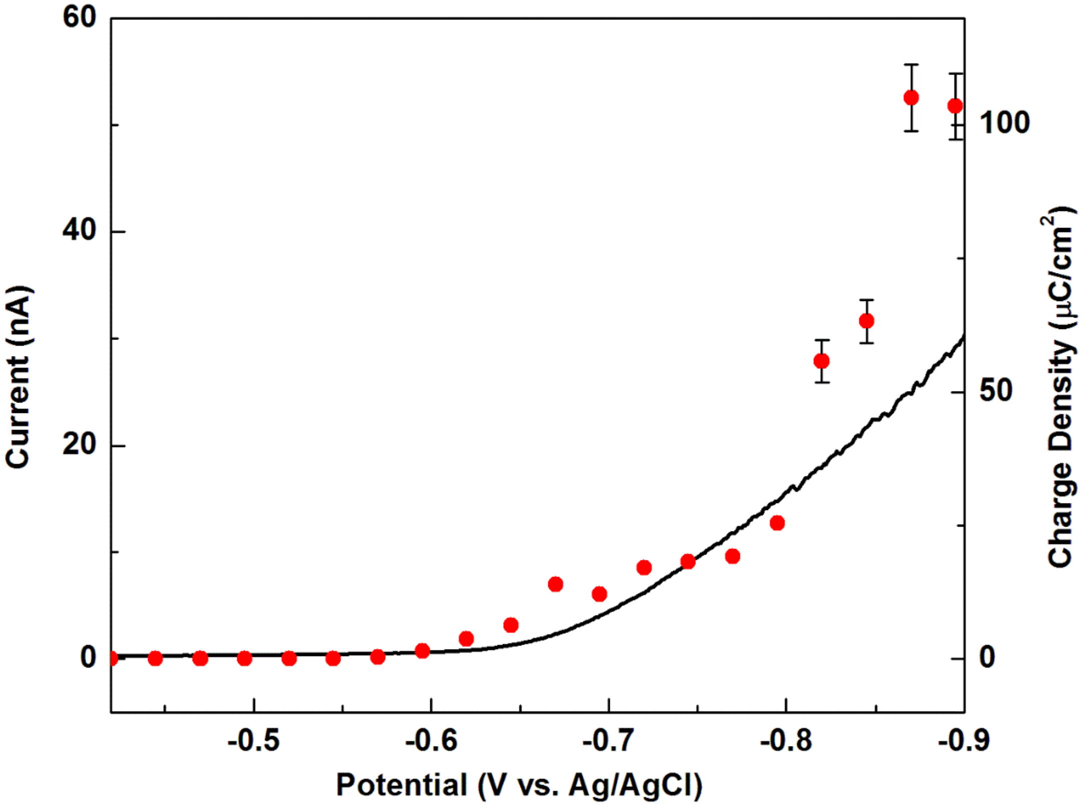

Figure S6. Zoomed in view of the MoS_2 surface redox titration curve. A reduction event observed in potentials -0.62 V to -0.8 V is attributed to the reduction of residual MoS_3 in the film.[2] Similar reduction event in the bulk of the film is also observed in the LSV shown in Figure S4.

Calculation of the Mo-H coverages at -0.92 V and -1.12 V

From the redox titration curve displayed in Figure 2 in the manuscript, the charge density obtained at -0.92 V is 196 µC/cm^2. Here, we take a similar amorphous catalyst surface of known metal atom density as a benchmark for the purposes of this calculation: CoP_i, with an overall surface formula of CoO_2 and a charge density due to cobalt redox of 270 µC/cm^2 (17 atoms/cm^2).[3,5] Because the charge density of CoP_i is based on a one-electron redox couple ($Co^{III/II}$) and that of MoS_2 based on a two-electron redox couple ($Mo^{IV/II}$), a benchmark charge density for full surface atom coverage will be 540 µC/cm^2 (270 µC/cm^2 * 2). Also the roughness factor (a measure of surface corrugation and porosity – measurement for a MoS_2 electrode is described above) difference must be taken into account: Rf, MoS_2 = 6 and Rf, CoP_i = 2.3.[5,7] Therefore with these considerations the hydride coverage for the MoS_2 electrode at -0.92 V is calculated as follows:

$$\mathbf{196\ \frac{\mu C}{cm^2} \times \frac{1}{540}\ \frac{cm^2}{\mu C}\ (for\ full\ coverage) \times \frac{2.3\ \ (Rf, CoP_i)}{6\ \ (Rf, MoS_2)}}$$

$$= \mathbf{0.139\,,\quad 14\,\%\ Mo\cdot H\quad Surface\ Coverage}$$

Similarly, the calculated hydride coverage at -1.12 V resulted in 31 %.

Measurement of the pseudo first-order HER rate constants

In the experimental setup concerned in this manuscript, the protons in solution are in excess compared to the surface generated Mo-H (0.1 M buffer strength, pH 4.6), therefore a pseudo first-order approximation can be made as follows.

$$\{MoS_2 \cdot \mathrm{H}\}^{2-} \quad + \quad H^+ \quad \rightarrow \quad MoS_2 \quad + \quad H_2$$

First-Order Rate Equation

$$\frac{d\{MoS_2 \cdot \mathrm{H}\}^{2-}}{dt} \;=\; -k'\{MoS_2 \cdot \mathrm{H}\}^{2-}$$

$$\ln[Mo \cdot H] \;=\; -k't \;+\; \ln[Mo \cdot H]_0$$

$$[Mo \cdot H] \quad [=] \quad mol \cdot m^{-2}$$

From the relationship above, a rate constant k' (equivalent to turnover frequency, TOF) can be extracted from a slope of the ln [Mo-H] vs. time plot (Figures 2 and 3). Note that [Mo·H] is a surface concentration, with units of mol·m^{-2}.

To ensure that the pseudo-first-order approximation in a buffered solution holds true, we have performed the same kinetic analysis at pH 5.3. Compared to that in pH 4.6, the proton concentration decreased by a factor of 5, and the resulting k' decreased by a factor of 5.8, in reasonable agreement with the predicted value. The results are summarized in Table S1 below.

Table S1. The pseudo-first-order kinetic rate constants of Mo-H HER determined at pHs 4.6 and 5.3. The expected rate decrease in lowered [H$^+$] suggests that the pseudo-first-order approximation in buffered solutions is reasonable.

pH	**[H$^+$] (mol/L)**	**k' (s^{-1})**	**[H+] ratio**	**k' ratio**
4.6 ± 0.1	2.5 x 10^{-5}	3.8 ± 1.2	5.0	5.8
5.3 ± 0.1	5.0 x 10^{-6}	0.65 ± 0.2		

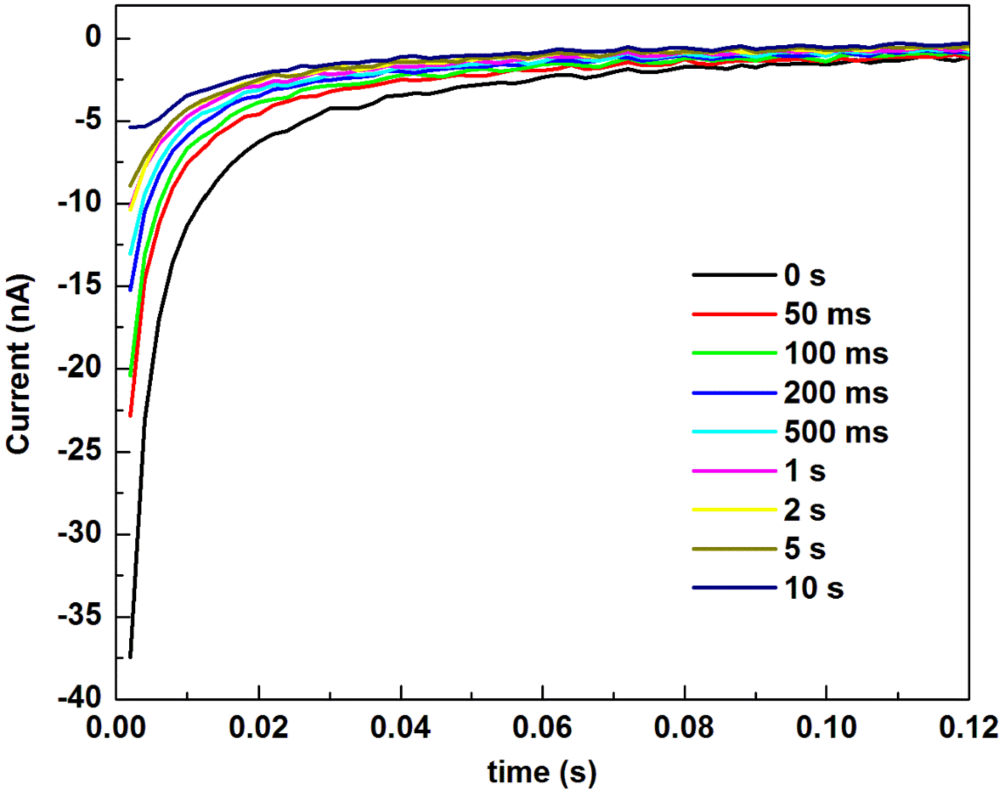

Figure S7. Titration chronoamperograms at -1.12 V with varying t_{delay}. A systematic decrease in the titration currents correspond to consumption of the active species Mo-H by the solvated protons via HER during the delay time. The integrated charge densities from this plot are plotted in Figure 3.

Collection of evolved H_2 as a function of t_{delay}

In order to confirm that the Mo-H titrated in this work is indeed an HER intermediate and the decay of which leads to H_2 evolution, an independent experiment was carried out in which the evolved H_2 (during t_{delay}, as Mo-H was being consumed) was collected. In the same experimental conditions as described in this work, the solution was replaced with buffered water in the absence of the redox mediator FcDM. The tip electrode was replaced to a Pt UME in order to collect (oxidize H_2) the product efficiently. Employing the same procedure as a SI-SECM experiment (a substrate pulse of 1 s was employed in order to avoid H_2 bubble formation), the substrate evolved H_2 was collected at the tip during t_{delay}. The amount of evolved H_2 was compared to the amount of consumed Mo-H at every t_{delay} (Figure S8); an excellent agreement between the two quantities suggest that the Mo-H is indeed an HER intermediate.

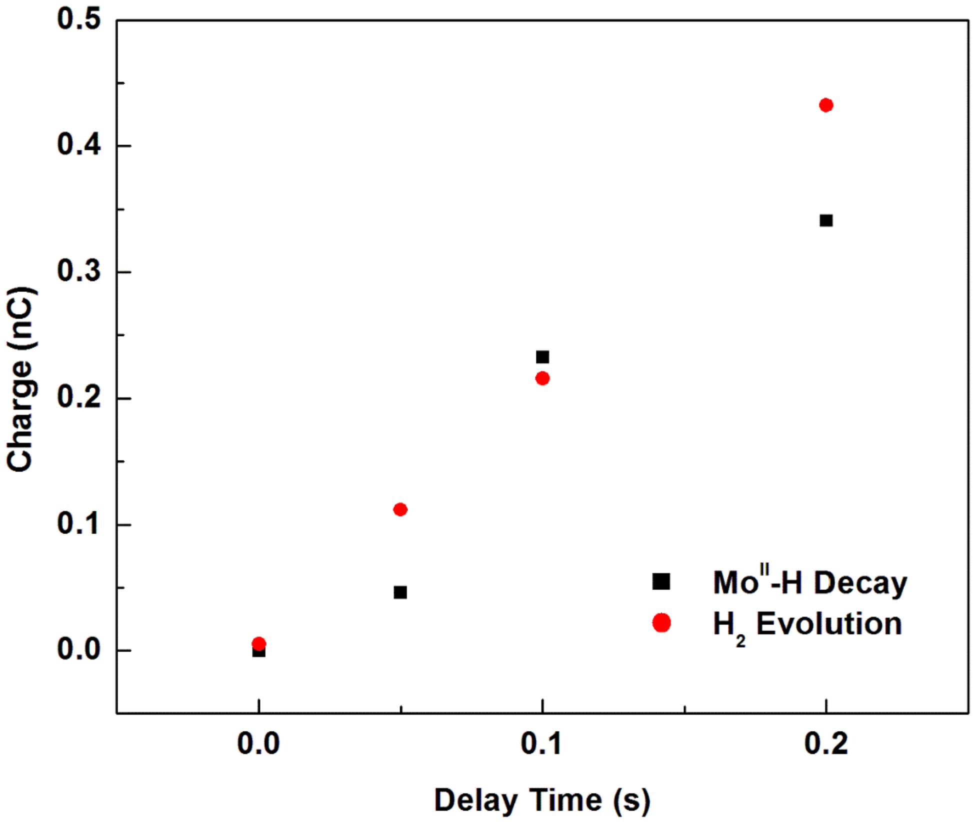

Figure S8. A plot of Mo-H decay and H_2 evolution as a function of t_{delay} (in pH 5.3, at 600 mV overpotential).

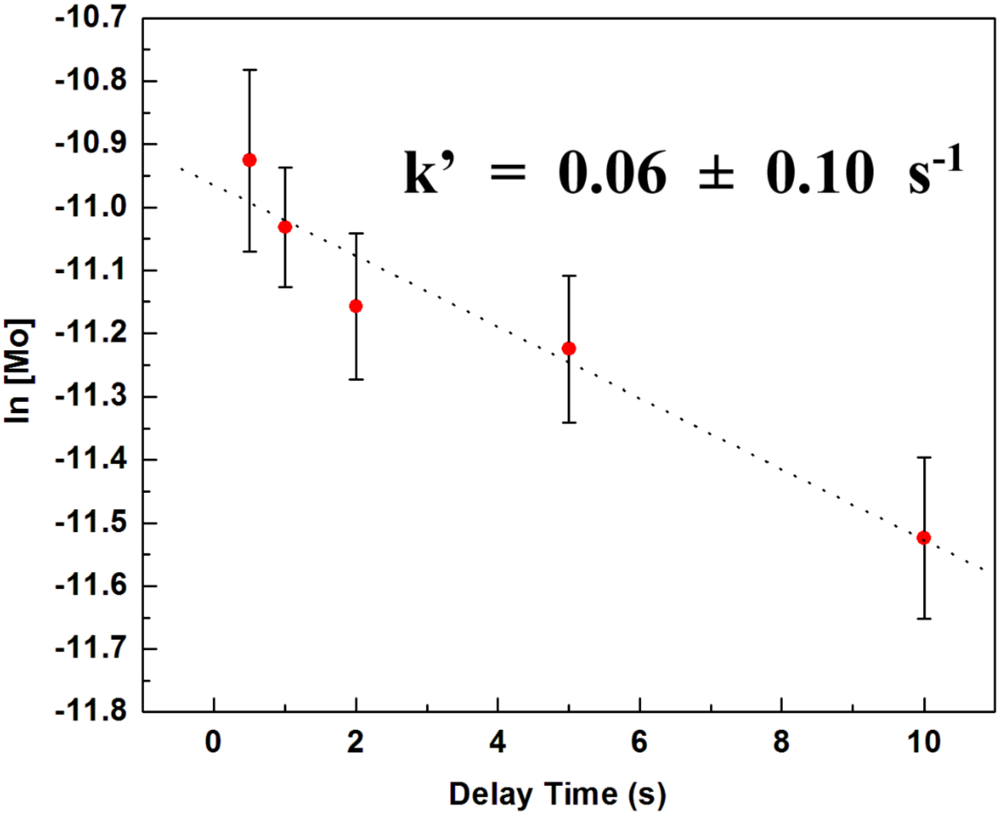

Figure S9. A plot of ln [Mo] vs. t_{delay} for $t_{delay} > 200$ ms (at substrate potential -1.12 V). A rate constant similar to that obtained at -0.92 V (14 % hydride coverage) was observed.

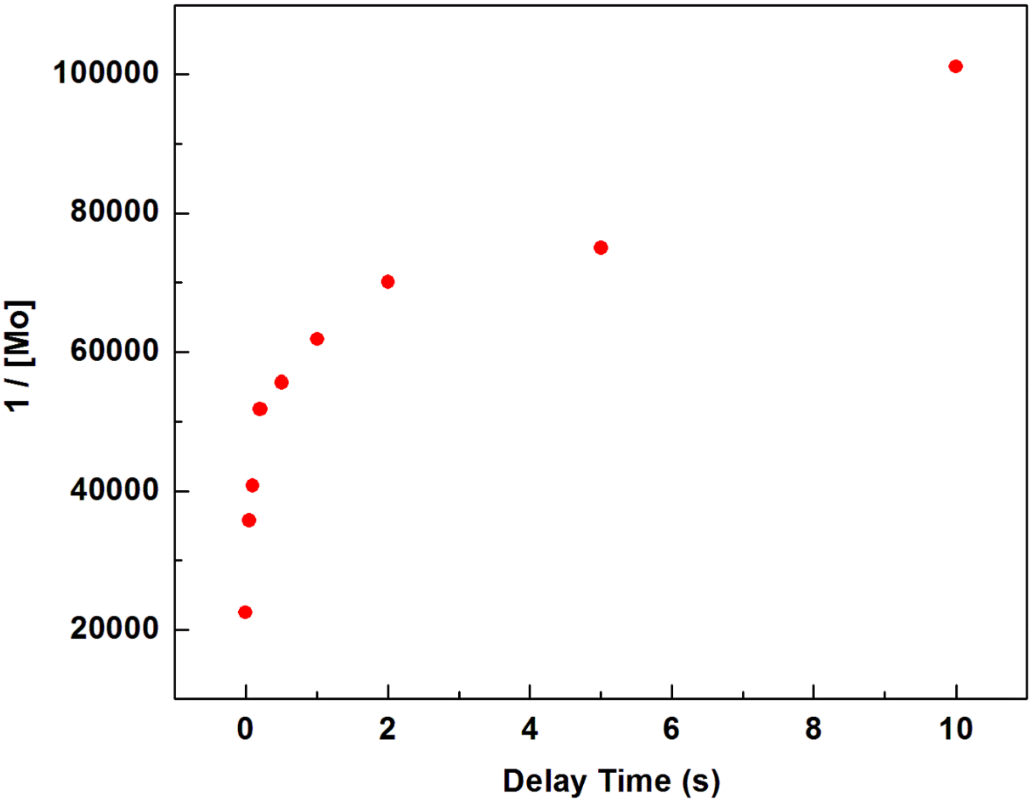

Figure S10. A plot of 1/[Mo] vs. t_{delay} at substrate potential -1.12 V. Non-linearity across all time ranges indicate that the reaction is not second order in Mo-H.

References

(1) Bard, A. J.; Mirkin, M. V. *Scanning Electrochemical Microscopy,* 2 ed.; CRC Press: Boca Raton, FL; 2012.

(2) Merki, D.; Fierro, S.; Vrubel, H.; Hu, X. Amorphous Molybdenum Sulfide Films as Catalysts for Electrochemical Hydrogen Production in Water. *Chem. Sci.* **2011**, *2*, 1262-1267.

(3) Ahn, H. S.; Bard. A. J. Switching Transient Generation in Surface Interrogation Scanning Electrochemical Microscopy and Time-of-Flight Techniques. *Anal. Chem.* **2015**, *87*, 12276-12280.

(4) Rodríguez-López, J.; Alpuche-Avilés, M. A.; Bard, A. J. Interrogation of Surfaces for the Quantification of Adsorbed Species on Electrodes: Oxygen on Gold and Platinum in Neutral Media. *J. Am. Chem. Soc.* **2008**, *130*, 16985-16995.

(5) Ahn, H. S.; Bard, A. J. Surface Interrogation of CoP_i Water Oxidation Catalyst by Scanning Electrochemical Microscopy. *J. Am. Chem. Soc.* **2015**, *137*, 612-615.

(6) Ahn, H. S.; Bard. A. J. Surface Interrogation Scanning Electrochemical Microscopy of $Ni_{1-x}Fe_xOOH$ ($0 < x < 0.27$) Oxygen Evolving Catalyst: Kinetics of the “fast” Iron Sites. *J. Am. Chem. Soc.* **2016**, *138*, 313-318.

(7) Ahn, H. S.; Tilley, T. D. Electrocatalytic Water Oxidation at Neutral pH by a Nanostructured $Co(PO_3)_2$ Anode. *Adv. Funct. Mater.* **2013**, *23*, 227-233.

(8) Levin, S.; Smith, A. L. Theory of the Differential Capacity of the Oxide/Aqueous Electrolyte Interface. *Discuss. Faraday Soc.* **1971**, *52*, 290-301.